A model for spectral diffusion induced by resonant energy migration applied to the 4A2→2E transition of Cr3+ in [Cr(ox)3]3- (ox = C2O42-)

Milos, Mia; Hauser, Andreas

How to cite

MILOS, Mia, HAUSER, Andreas. A model for spectral diffusion induced by resonant energy migration applied to the 4A2→2E transition of Cr3+ in [Cr(ox)3]3- (ox = C2O42-). In: Journal of luminescence, 2009, vol. 129, n° 12, p. 1901–1904. doi: 10.1016/j.jlumin.2009.04.093

This publication URL: https://archive-ouverte.unige.ch/unige:6165
Publication DOI: 10.1016/j.jlumin.2009.04.093

Journal of Luminescence 129 (2009) 1901–1904

Contents lists available at ScienceDirect

Journal of Luminescence

journal homepage: www.elsevier.com/locate/jlumin

A model for spectral diffusion induced by resonant energy migration applied to the $^4A_2 \rightarrow {}^2E$ transition of Cr^{3+} in $[Cr(ox)_3]^{3-}$ ($ox = C_2O_4^{2-}$)

Mia Milos, Andreas Hauser *

Département de chimie physique, Université de Genève, Bâtiment de Science 2, 30 quai Ernest-Ansermet, CH-1211 Genève 4, Switzerland

ARTICLE INFO

Available online 20 May 2009

Keywords:
Energy migration
Spectral diffusion
Fluorescence line narrowing
Chromium(III)-*tris*-oxalate

ABSTRACT

In the 3D oxalate networks $[NaCr(ox)_3][Rh(bpy)_3]ClO_4$ and $[NaCr(ox)_3][Ru(bpy)_3]$ (ox = oxalate, bpy = 2,2′-bipyridine) three different types of energy migration within the $^4A_2 \rightarrow {}^2E$ transition can be identified. One is a resonant process between spectral members spaced by the ground-state zero-field splitting (ZFS). This leads to the sequential appearance of additional sharp lines spaced by the ground-state ZFS in the fluorescence line narrowing spectrum across the inhomogeneous line. The second one is a quasi-resonant process between spectral neighbours and manifests itself by rapid spectral diffusion. The third one is the well-known phonon-assisted process setting in at higher temperature.

1. Introduction

Excitation energy transfer between a donor and an acceptor and energy migration among identical chromophores play an important role in many areas of physics, chemistry, and biology [1–3]. The $^4A_2 \rightarrow {}^2E$ spin–flip transition of Cr^{3+} in an octahedral or nearly octahedral environment is instrumental for an in depth understanding of the parameters governing the latter [4,5]. The three-dimensional oxalate networks $[NaCr(ox)_3][Ru(bpy)_3]$ and $[NaCr(ox)_3][Rh(bpy)_3]ClO_4$ [6], with their high chromophore concentrations and insignificant exchange interactions between chromophores, have several advantages for their study compared to ruby and other doped systems [5,7,8]. In fact, they allow a clear distinction between different mechanisms for energy migration as depicted in Fig. 1 [9]. Fluorescence line narrowing (FLN) spectroscopy showed that at cryogenic temperatures, where phonon-assisted energy migration is negligible, two different types of resonant energy migration may take place. One is a resonant process between spectral members spaced by the ground-state zero-field splitting (ZFS). This leads to the sequential appearance of additional sharp lines spaced by the ground-state ZFS in the FLN spectrum across the inhomogeneous line [10]. The second one is a quasi-resonant process between spectral neighbours and manifests itself by rapid spectral diffusion [9]. The third one is the well-known phonon-assisted process setting in at higher temperature. In the following, we will first develop a simple model for spectral diffusion resulting from energy migration, and then go on to discuss experimental results obtained on the above-mentioned oxalate networks.

2. Spectral diffusion, the model

At low temperatures the homogeneous line width Γ_{hom} of an electron origin is often much smaller than the inhomogeneous line width $\Gamma_{inh.}$ For the above-mentioned fully concentrated oxalate networks Γ_{hom} is typically $0.02\,cm^{-1}$ (600 MHz) at 1.5 K, whereas Γ_{inh} varies from 1 to $4\,cm^{-1}$ depending upon the exact composition [9]. At low temperatures, where phonon-assisted processes are frozen, resonant and quasi-resonant energy migration may still occur because of the high concentration of chromophores. In the absence of exchange interactions, these processes are based on electric dipole–electric dipole interaction between the respective transition dipole moments [11]. The probability for an energy transfer process is given by

$$w_{DA} = \frac{1}{\tau_D}\left(\frac{R_c}{R_{DA}}\right)^6 \tag{1}$$

with the critical radius [12]

$$R_c = \left(Const \times \frac{\kappa^2 f_A \Omega_{DA} \eta_D^r}{\tilde{\nu}_{DA}^4}\right)^{1/6} \tag{2}$$

at which w_{DA} is equal to the intrinsic decay $k_D = \tau_D^{-1}$. In Eq. (2), f_A is the dimensionless oscillator strength of the acceptor transition, η_D^r the luminescence quantum efficiency of the donor transition, $\tilde{\nu}_{DA}$ the mean energy at which the transfer takes place, κ^2 a geometrical factor, which averaged over all possible orientations takes on a value of 2/3, *Const* regroups fundamental quantities and takes on a value of $\sim 10^{31}$ for $\tilde{\nu}_{DA}$ in cm^{-1} and R_c in Å. The spectral overlap integral of the normalised line shape functions of the donor emission, g_D, and the acceptor absorption,

---

* Corresponding author. Tel.: +41 22 379 6559; fax: +41 22 379 6103.
E-mail address: andreas.hauser@unige.ch (A. Hauser).

0022-2313/$ - see front matter © 2009 Elsevier B.V. All rights reserved.
doi:10.1016/j.jlumin.2009.04.093

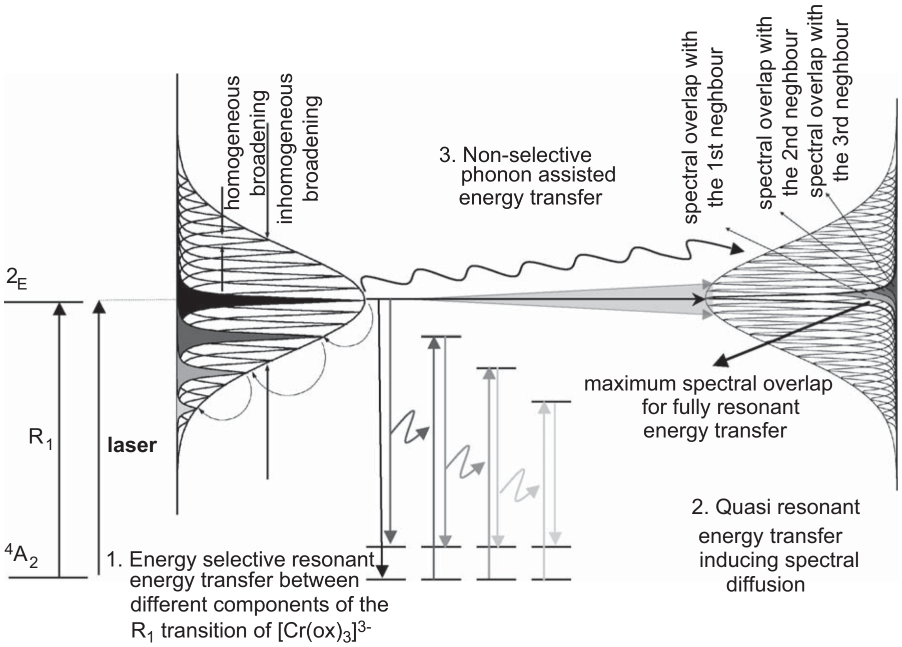

Fig. 1. Schematic presentation of the three mechanisms for energy migration at high chromophore concentrations. (1) Resonant energy transfer between different components of the ground state. (2) Quasi-resonant energy migration between spectral neighbours resulting in spectral diffusion around the resonant line and (3) non-energy selective phonon-assisted energy migration at elevated temperature [9].

g_A, is given by

$$\Omega_{DA} = \int g_A(\tilde{\nu}) g_D(\tilde{\nu})\, d\tilde{\nu} \tag{3}$$

For energy migration, this has to be taken between the two homogeneous lines either fully resonant for chromophores with exactly the same central frequency, or quasi-resonant with partial spectral overlap for spectral neighbours as shown in Fig. 1. For two Lorentzian lines of equal width centred at $\tilde{\nu}_D$ and $\tilde{\nu}_A$, respectively, the overlap integral is given by [13]

$$\Omega_{DA} = \frac{1}{\pi} \frac{\Gamma_{hom}}{\Gamma_{hom}^2 + (\tilde{\nu}_D - \tilde{\nu}_A)^2} \tag{4}$$

For the fully resonant case, this simplifies to $\Omega_{DA} = 1/\pi\Gamma_{hom}$. For $\Gamma_{hom} \approx 0.02\,cm^{-1}$, this results in a maximum value of $\Omega_{DA} \approx 16\,cm$ and of $R_c \approx 34\,Å$ [9]. The mean number of chromophores, n_m, resonant within one homogeneous line width with a donor at the centre of the inhomogeneous distribution within a sphere of radius R_c is given by

$$n_m = \frac{2\Gamma_{hom}}{\Gamma_{inh}} N_{tot} \frac{4\pi}{3} R_c^3 \sim \frac{\sqrt{\Gamma_{hom}}}{\Gamma_{inh}} \tag{5}$$

For $\Gamma_{inh} \approx 1\,cm^{-1}$, n_m can be estimated to be >6, for $\Gamma_{inh} \approx 4$ cm^{-1} it falls to <2 [9]. Thus at a narrow enough inhomogeneous line width, $\Sigma w_{DA} \gg k_D$, where the sum includes all potential acceptors for a given donor.

For computational purposes the continuous distribution of chromophores in the inhomogeneous distribution is divided into n closely spaced discrete sets. In principle, each donor has a different environment of potential acceptors and therefore a different energy transfer probability to members of the sets with which it has non-negligible spectral overlap. For simplicity, an average energy transfer rate constant is assumed, in which case the population of the excited state in set i following pulsed excitation into set i_0 is given by n coupled

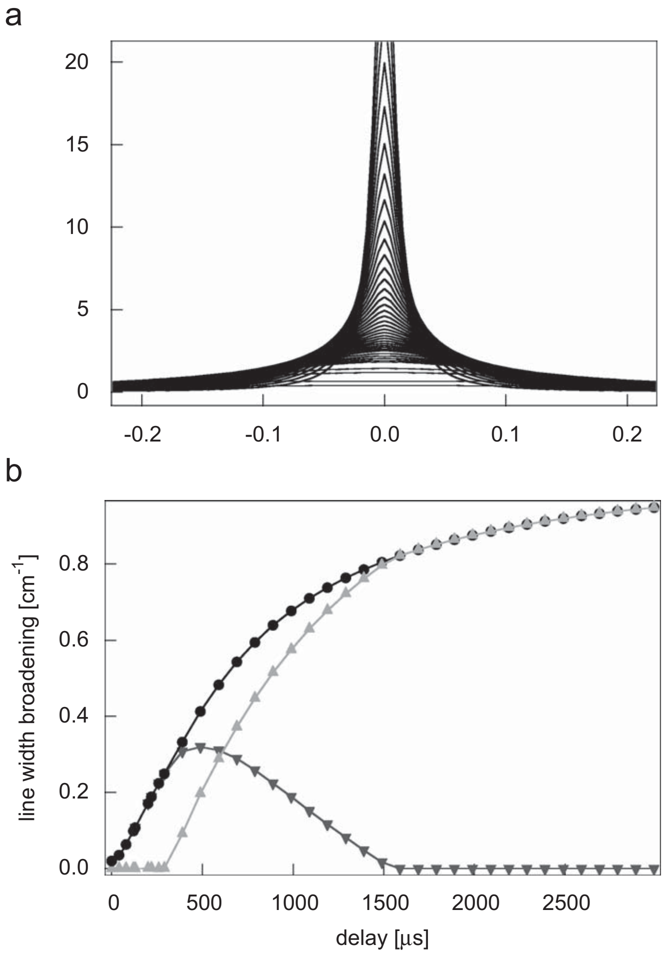

Fig. 2. (a) Evolution of the emission band shape as function of delay following pulsed laser excitation through spectral diffusion due to energy migration and (b) full-width at half-maximum and decomposition into Lorentzian and Gaussian contributions.

differential equations

$$\frac{\mathrm{d}N_{\mathrm{ei}}}{\mathrm{d}t} = -\left(k_{\mathrm{D}} + k_{\mathrm{ET}}\sum_{j}\Omega_{i,j}N_{\mathrm{g}j}\right)N_{\mathrm{ei}} + k_{\mathrm{ET}}\sum_{j}\Omega_{j,i}N_{\mathrm{g}i}N_{\mathrm{e}j} \quad i = 1, 2, \ldots, n \tag{6}$$

N_{ei} is the number of centres of the ith set in the excited state, $N_{\mathrm{g}i}$ the corresponding ground-state population, k_{ET} is related to the energy transfer probability, and the $\Omega_{i,j}$ describe all possible spectral overlap integrals according to Eq. (4). For weak excitation $N_{\mathrm{ei}} \ll N_{\mathrm{g}i}$, the $N_{\mathrm{g}i}$ are constant and are given by the inhomogeneous Gaussian distribution function. In this case, the set of differential equations becomes linear and can be solved numerically for $N_{\mathrm{e}i}(t)$ using the starting condition that at $t = 0$, $N_{\mathrm{ei} \neq i_0} = 0$ and $N_{\mathrm{ei}_0} = N_0$. Finally, the evolution of the band shape can be calculated by the weighted sum of Lorentzians

$$f(\tilde{\nu}, t) = \sum_{i} \frac{1}{\pi} \frac{\Gamma_{\mathrm{hom}}/2}{(\tilde{\nu} - \tilde{\nu}_i)^2 + (\Gamma_{\mathrm{hom}}/2)^2} N_{\mathrm{e}i}(t) \tag{7}$$

Fig. 2a shows the calculated evolution of the band profile and Fig. 2b the full-width at half-maximum as a function of delay following pulsed excitation at the centre of the inhomogeneous distribution. For the sample calculation, $\Gamma_{\mathrm{inh}} = 1.0\,\mathrm{cm}^{-1}$, $\Gamma_{\mathrm{hom}} = 0.02\,\mathrm{cm}^{-1}$, $k_{\mathrm{D}} = 700\,\mathrm{s}^{-1}$, and k_{ET} was set to such a value that the maximum value of Σw_{DA} at the centre of the distribution is $10^5\,\mathrm{s}^{-1}$. Evidently, the band broadens quickly, initially keeping its Lorentzian shape, but as the width becomes larger, it first evolves into a Voigt profile and finally ends in the Gaussian profile of the inhomogeneous distribution. The decomposition into Lorentzian and the Gaussian contributions to the profile is included in Fig. 2b.

3. Energy migration within the ^{2}E state of Cr^{3+}

Fig. 3a shows time-resolved FLN spectra for [NaCr(ox)$_3$][Ru(bpy)$_3$] at 1.4 K for irradiation into the maximum of the lower energy component of the R1 line of the $^4\mathrm{A}_2 \rightarrow {}^2\mathrm{E}$ transition. At the shortest delay the spectrum consists of the normal three lines spaced by the ground-state ZFS of 1.3 cm^{-1} also observed for dilute systems in the absence of energy migration [14,15]. But already at comparatively short delays, the three lines broaden out rapidly and additional satellite lines appear on both sides also spaced by the ground-state ZFS. The latter are due to energy transfer involving the transitions to the upper level of the ground state of the donor and from the lower level of the acceptor such that within the inhomogeneous distribution the two have the same energy, and vice versa. The rapid broadening, as displayed in Fig. 4 is due to quasi-resonant transfer between spectral neighbours within the inhomogeneous band as described above. This is borne out by comparison with the FLN spectra of [NaCr(ox)$_3$][Rh(bpy)$_3$](ClO$_4$)$_2$ at 1.4 K shown in Fig. 3b and c. The difference between the two compounds lies in the inhomogeneous widths, which are 1.1 cm^{-1} for the former and 4.2 cm^{-1} for the latter. Thus, for the latter the concentration of resonant and quasi-resonant species is considerably smaller and therefore the temporal broadening of the lines in the FLN spectra does not much exceed the spectral resolution of 0.25 cm^{-1} of the

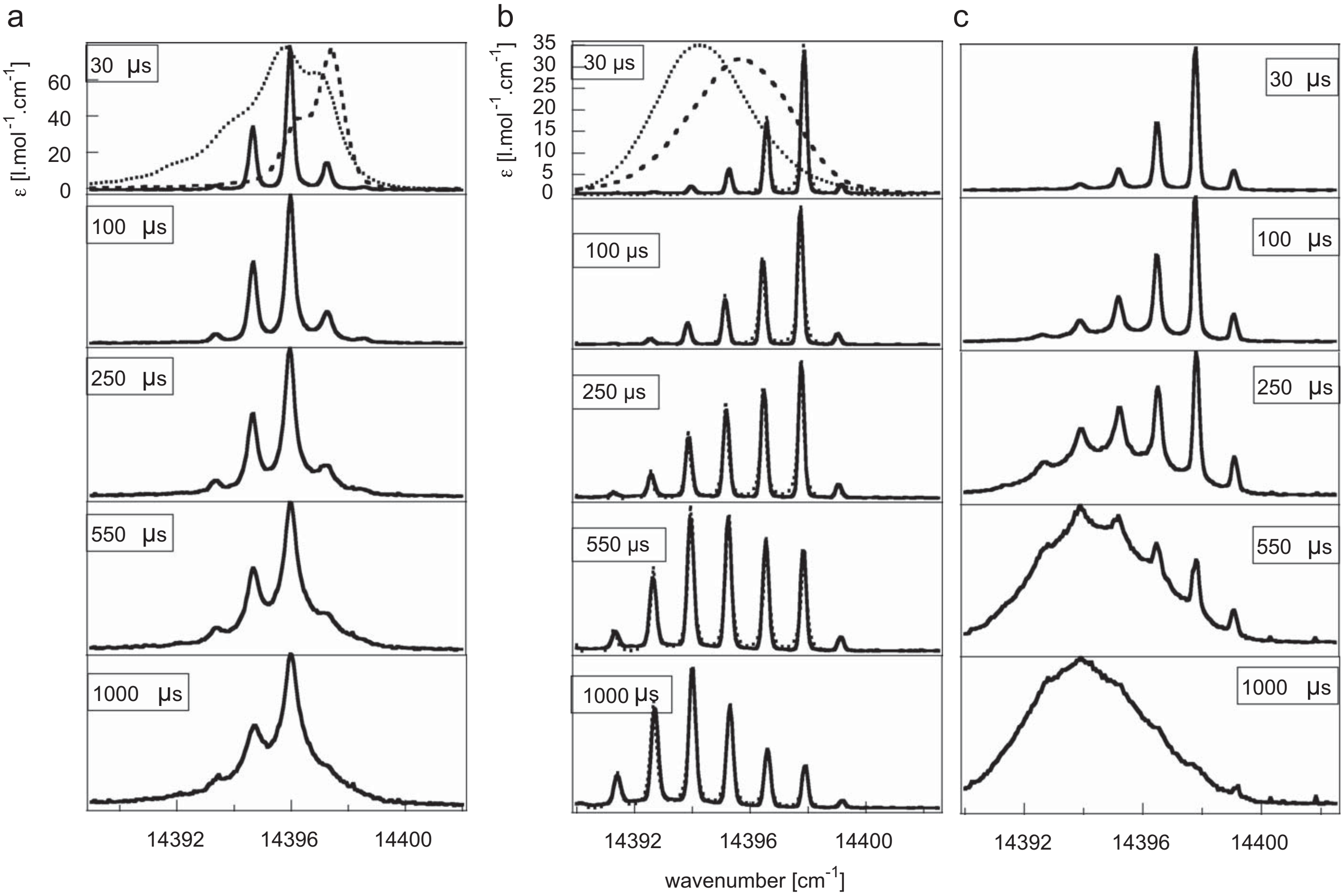

Fig. 3. (a) Time-dependant FLN spectra of [NaCr(ox)$_3$][Ru(bpy)$_3$] at 1.4 K after excitation into the R1 line of the $^4\mathrm{A}_2 \rightarrow {}^2\mathrm{E}$ transition at 14396.0 cm^{-1}. (b) Time-dependant FLN spectra of [NaCr(ox)$_3$][Rh(bpy)$_3$](ClO$_4$)$_2$ at 1.4 K after excitation at 14397.8 cm^{-1}, and (c) at 3.2 K. The absorption and non-selective luminescence spectra are included for comparison.

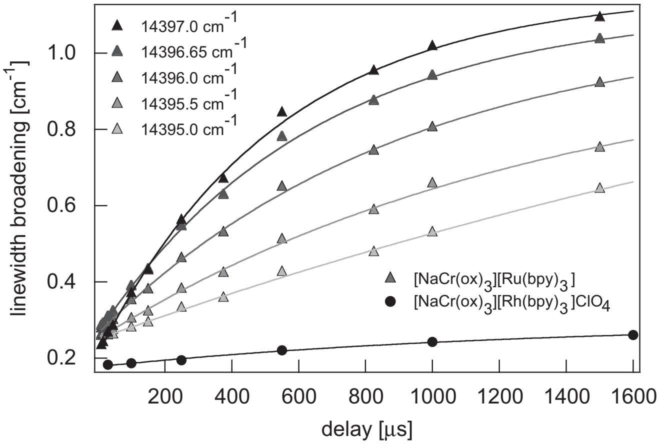

Fig. 4. Evolution of the observed bandwidth of the individual sharp lines as function of time following pusled excitation for $[NaCr(ox)_3][Ru(bpy)_3]$ (▲) at different wavelengths across the inhomogeneous distribution and for (●) $[NaCr(ox)_3][Rh(bpy)_3](ClO_4)_2$, $T = 1.4$ K.

detection system. However, as more multiples of the ZFS of $1.3\,cm^{-1}$ can be accommodated within the inhomogeneous width of $4.2\,cm^{-1}$, the number of satellites appearing with a spacing of the ZFS is larger. The fact that no inhomogeneous background appears at longer delays also proves that the phonon-assisted process is frozen at 1.4 K. At 3.2 K, however, the phonon-assisted process becomes important as shown for $[NaCr(ox)_3][Rh(bpy)_3](ClO_4)_2$ in Fig. 3c. The signature of the phonon-assisted process is clearly very different from the spectral diffusion observed for the system with the narrower inhomogeneous distribution of Fig. 3a.

4. Conclusions

Three different energy migration processes have been clearly distinguished by FLN spectroscopy in three-dimensional oxalate network compounds. $[NaCr(ox)_3][Ru(bpy)_3]$ having a 4 times smaller inhomogeneous line width than $[NaCr(ox)_3][Rh(bpy)_3]ClO_4$, has more resonant chromophores inside the critical sphere than the latter provided the homogeneous line widths are the same. This has consequences for the rate of resonant energy migration in those compounds, making it considerably faster in case of $[NaCr(ox)_3][Ru(bpy)_3]$. With a simple model based on Förster's electric dipole–dipole energy transfer and taking into account all the possible spectral overlap integrals that one chromophore can have with its spectral neighbours, it is possible to simulate the spectral diffusion in accordance with experimental observation. Fitting the time evolution of the band with a Voigt profile, one notes that the line shape evolves from a Lorentzian function at short delays to a Gaussian distribution limited by the inhomogeneous line width. A key parameter in the model is the homogeneous line width. Thus the question is whether the homogeneous line widths are the same for the two slightly different compounds. In order to clarify this, further experiments will include transient spectral hole burning on $[NaCr(ox)_3][Ru(bpy)_3]ClO_4$ and $[NaCr(ox)_3][Ru(bpy)_3]$ as well as $[NaCr(ox)_3][Zn(bpy)_3]$.

Acknowledgement

We thank the Swiss National Science Foundation for the financial support of this work.

References

[1] Advanced solid state lasers, in: M.M. Fejer, H. Injeyan, U. Keller (Eds.), in: OSA Trends in Optics and Photonics, vol. 26, Optical Society of America, Washington, 1999.
[2] T. Justel, H. Nikol, C. Ronda, Angew. Chem., Int. Ed. 37 (1998) 3084.
[3] M. Gratzel, Nature (London, UK) 414 (2001) 338.
[4] S. Decurtins, H.W. Schmalle, R. Pellaux, P. Schneuwly, A. Hauser, Inorg. Chem. 35 (1996) 1451.
[5] G.F. Imbusch, Phys. Rev. 152 (1967) 326.
[6] S. Decurtins, H.W. Schmalle, P. Schneuwly, J. Ensling, P. Guetlich, J. Am. Chem. Soc. 116 (1994) 9521.
[7] S.A. Basun, R.S. Meltzer, G.F. Imbusch, J. Lumin. 125 (2007) 31.
[8] Z. Hasan, S.T. Keany, N.B. Manson, J. Phys. C: Solid State Phys. 19 (1986) 6381.
[9] M. Milos, S. Kairouani, S. Rabaste, A. Hauser, Coord. Chem. Rev. (2008).
[10] A. Hauser, M.E. von Arx, V.S. Langford, U. Oetliker, S. Kairouani, A. Pillonnet, Top. Curr. Chem. 241 (2004) 65.
[11] T. Forster, Ann. Phys. [6 Folge] 2 (1948) 55.
[12] B. Henderson, G.F. Imbusch, Clarendon Press, Oxford, 1989.
[13] B. Di Bartolo, X. Chen (Eds.), Advances in Energy Transfer Processes, World Scientific, New Jersey, 2001.
[14] M.E. von Arx, A. Hauser, H. Riesen, R. Pellaux, S. Decurtins, Phys. Rev. B: Condens. Matter 54 (1996) 15800.
[15] A. Hauser, H. Riesen, R. Pellaux, S. Decurtins, Chem. Phys. Lett. 261 (1996) 313.